J. Hydrol. Hydromech., 62, 2014, 1, 24–32
DOI: 10.2478/johh-2014-0011

Wavelet based deseasonalization for modelling and forecasting of daily discharge series considering long range dependence

Elena Szolgayová[*1], Josef Arlt[2], Günter Blöschl[3], Ján Szolgay[4]

[1]The Centre for Water Resource Systems, Vienna Universtity of Technology, Karlsplatz 13, 1040, Vienna, Austria.
[2]University of Economics, Faculty of Informatics and Statistics, nám. W. Churchilla 4, 130 67, Prague, Czech Republic.
[3]Institute of Hydraulic Engineering and Water Resources Management, Vienna University of Technology, Karlsplatz 13, 1040, Vienna, Austria.
[4]Slovak University of Technology, Radlinského 11, 813 68, Bratislava, Slovakia.
[*]Corresponding author. E-mail: szolgayova@waterresources.at

Abstract: Short term streamflow forecasting is important for operational control and risk management in hydrology. Despite a wide range of models available, the impact of long range dependence is often neglected when considering short term forecasting. In this paper, the forecasting performance of a new model combining a long range dependent autoregressive fractionally integrated moving average (ARFIMA) model with a wavelet transform used as a method of deseasonalization is examined. It is analysed, whether applying wavelets in order to model the seasonal component in a hydrological time series, is an alternative to moving average deseasonalization in combination with an ARFIMA model. The one-to-ten-steps-ahead forecasting performance of this model is compared with two other models, an ARFIMA model with moving average deseasonalization, and a multiresolution wavelet based model. All models are applied to a time series of mean daily discharge exhibiting long range dependence. For one and two day forecasting horizons, the combined wavelet – ARFIMA approach shows a similar performance as the other models tested. However, for longer forecasting horizons, the wavelet deseasonalization - ARFIMA combination outperforms the other two models. The results show that the wavelets provide an attractive alternative to the moving average deseasonalization.

Keywords: Daily streamflow; Wavelets; ARFIMA; Deseasonalization; Long range dependence; Forecasting.

INTRODUCTION

Short term forecasting is important in operational hydrology for reservoir operations and risk control (Hipel and McLeod, 1994). There are several approaches for short term modelling of daily discharges, including deterministic conceptual rainfall–runoff models (Blöschl et al.,1997; Reszler et al., 2008) and a wide range of stochastic models, such as autoregressive (Burlando et al., 1993, Quimpo, 1969) or regime switching models (Komorník et al., 2006; Komorníková et al., 2008) or neural networks (Maier and Dandy, 2000; Nelson, 1999; Zealand et al., 1999).

Removing systematic components (trend and seasonality) in the process of time series modelling is a part of the standard time series modelling paradigm (Box and Jenkins, 1976). The seasonality of streamflows stems from the earth rotation and can be explained by the physical processes in the catchment, such as snowmelt and precipitation. Therefore it is often removed in stochastic streamflow modelling (Komorník et al., 2006; Komorníková et al., 2008; Prass et al., 2012). Thus deseasonalization simplifies time series modelling and forecasting and possibly widens the model choice. There are numerous studies elaborating on the stochastic part of the model; for example see Koop et al. (1997), Montanari et al. (1997), Ooms and Franses (2001); however studies focusing on deseasonalisation are lacking.

Despite the huge range of models available, the impact of long range dependence is often neglected in modelling in hydrological time series. However, Prass et al. (2012) found that long range dependence may have an impact on the performance of time series models with short time step. Moreover incorporating long range dependence into time series modelling is also conceptually important, since the model should capture the behaviour of the data as realistically as possible. Long range dependent processes are characterized by hyperbolic decrease of the autocorrelation function and are closely related to self-similarity (Doukhan et al., 2003). Long range dependence has been encountered in various hydrological (Ehsanzadeh and Adamowski, 2010; Koscielny-Bunde et al., 2006; Lye and Lin, 1994; Pelletier and Turcotte, 1997) and other data. Autoregressive fractionally integrated moving average (ARFIMA, (Beran, 1994)) models are a tool often used for the modelling of long range dependent time series (Lohre et al., 2003; Montanari et al., 1997; Prass et al., 2012).

The presence of periodic or seasonal components generally has an effect on long range dependence estimation (Montanari et al., 1999). However, the possibility of improving the deseasonalization step in the modelling process is scarcely discussed, even though each deseasonalization method has an effect on the covariance structure of the resulting time series, thus influencing the Hurst coefficient and the following model parameters.

Wavelet decomposition is a popular tool used to model and forecast (Renaud et al., 2003; Starck et al., 1998) periodic behaviour of time series. In hydrology, wavelets are scarcely used for forecasting (Adamowski, 2008) and wavelet modelling in hydrology is done especially in combination with neural networks (Renaud et al., 2003; Thuillard, 2002; Wei et al., 2012; Yousefi et al., 2005). In general, more attention is paid to feature extraction and detailed process description (Andreo, 2006; Grinsted et al., 2004; Pasquini and Depetris, 2010; Torrence and Compo, 1998) rather than to their potential to be employed for deseasonalization.

Since wavelets are able to capture the changes in a given frequency interval over time, they thus make it possible to

describe the changes in the annual cycle of the discharge time series as a reaction to its driving processes such as precipitation. It seems this would be a process more based approach to the deseasonalization of the discharge time series than the moving averages deseasonalization method.

The main objective of this study is, therefore, to examine, whether applying wavelets in order to model the seasonal component in a hydrological time series is an alternative to moving average deseasonalization in combination with a long-range dependent ARFIMA model. To examine the potential of the approach for practical applications, three models will be compared through their actual one to ten steps ahead forecasting performance. The following questions will be analysed: What are the effects of deseasonalization on the model fit and forecasting performance in a daily discharge time series with long range dependence? How is the model prediction performance affected by the alternative deseasonalization procedure? Is wavelet decomposition a suitable method for removing the seasonal component of daily discharge series?

In order to address these questions we adjust the standard modelling concept (Box and Jenkins, 1976) by replacing the generally used moving average seasonal filter by a wavelet filter, thus obtaining a combined wavelet – an ARFIMA model. This will be applied to a series of daily river discharges from Lower Austria and a one-to-ten-steps-ahead forecasts will be compared with a classical model combining the removal of seasonal components via moving averages smoothing and an ARFIMA model and a purely wavelet based model.

METHODS

In order to assess the impact of removing the seasonal components from a time series on model fit and forecasting, three different models will be considered. An overview can be seen on Fig. 1.

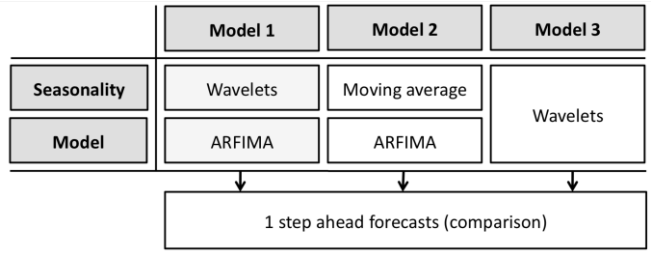

Fig. 1. Analysis overview.

The first model uses a suitable frequency interval to remove the most significant seasonal components by wavelet decomposition and fits an ARFIMA model to the residuals. In the second model, the standard approach combining a moving average deseasonalization with an ARFIMA model is applied. The last approach is based on wavelet decomposition and a multiresolution model according to Renaud et al. (2003). In general, the modelling procedure for the first two models is as follows:

1. Removing trend and seasonality;
2. Fitting the ARFIMA (p,d,q) model;
3. One-to-ten steps ahead forecasts construction.

In the last model, steps 1 and 2 are replaced by wavelet decomposition and a multiresolution model. A description of the applied models follows in the next sections. A description of the underlying mathematical background including a definition of long range dependent time series and the ARFIMA model can be found in Appendix 1.

Discrete wavelet transform and predictions

Using multiresolution wavelet analysis, a signal can be approximated by

$$X_t \approx \sum_k s_{J,k}\phi_{J,k}(t) + \sum_{j=1}^{J}\sum_k d_{j,k}\psi_{j,k}(t) \quad (1)$$

where $\psi_{j,k} = 2^{-j/2}\psi(2^{-j}t - k)$ are functions obtained by translations and dilations of a mother wavelet $\psi(t)$, $\phi_{J,k} = 2^{-J/2}\phi(2^{-J}t-k)$ is obtained analogically from a father wavelet $\varphi(t)$, $s_{j,k}, d_{j,k}$ are the wavelet transform coefficients and J is an integer. In general it holds $\int_{\Re}\psi(t)dt = 0$ and $\int_{\Re}\phi(t)dt = 1$. Furthermore the family of functions $\psi(2^{-j}t-k)$, $j,k \in \boldsymbol{Z}$ form a basis of the $L^2(\Re)$ space. The parameters j,k localize the wavelet in frequency and time. For further properties of the wavelet functions see e.g. Starck et al. (1998). Eq. 1 can be shortly rewritten as

$$X_t \approx S_{J,t} + \sum_{j=1}^{J} D_{j,t} \quad (2)$$

with $S_{J,t} = \sum_k s_{J,k}\phi_{J,k}(t)$ being the smooth signal and $D_{j,t} = \sum_k d_{j,k}\psi_{j,k}(t)$ being the detail signals for the frequency interval $(2^{-j-1}, 2^{-j})$.

For more details on the properties of the wavelet transform see e.g. Mallat (1998), Shensa (1992) or Starck et al. (1998). There are several methods in the literature dealing with the implementation of discrete wavelet transform (Gencay et al., 2001; Shensa, 1992; Starck et al., 1998). In model one, forecasting from the resolution level containing the annual periodicity of the detail signal $D_{j,t}$ is needed. On the other hand in model three, $D_{j,t}$, $S_{J,t}$ for all $j = 1, \ldots, J$ are necessary for a forecast calculation. For this reason, two different methods are applied in the data analysis.

Description of the models

Model one

The maximum overlap discreet wavelet transform (MODWT) (Gencay et al., 2001) with the least asymmetric wavelet of order eight is be applied for modelling the seasonal component in model one. This wavelet cannot be given in a closed form and the coefficients are calculated iteratively. For details see Daubechies (1992).

The forecasts $X_{T+s+1}, \ldots, X_{T+s+h}$, $s = 0, \ldots$ for the observed time series $X_1, \ldots, X_{T+s}$ are calculated in following steps

- A wavelet transform of the time series $X_{s+1}, \ldots, X_{T+s}$ is performed. Starting at X_{s+1} implies that the length of the transformed time series is always constant, thus the annual periodicity is being maintained at each time step. In general, a disadvantage of the MODWT algorithm is the presence of edge effects due to the circular shift of the time series, possibly causing significant inconsistencies in the forecasted seasonal component.

A trigonometric function to the wavelet coefficients is fitted followed by the inverse transform in order to obtain the forecasts of the seasonal component (Yousefi et al., 2005). A two stage linear least squares fit (Dou and Chan, 1998) is used to estimate the trigonometric function. In the first step a linear problem is solved where the phase shift and amplitude of a sinusoidal function are fitted; in the second step the frequency of the signal is estimated by

$$\min_{\omega}\{\min_{A,\theta} J_{\omega}(A,\theta)\} \quad (3)$$

where $J_{\omega}(A,\theta)=\sum_{t=0}^{T+s}(X_t - A\sin(\omega t+\theta))^2$, A is the amplitude, ω the frequency and θ the phase shift of the signal.

- The time series is deseasonalized. The h-step-ahead forecast from the deseasonalized time series using the ARFIMA model is calculated.
- The forecast of the seasonal component obtained as indicated in previous steps is then added to the ARFIMA forecast in order to obtain the overall model forecast for the days $X_{T+s+1},...X_{T+s+h}$.

Model two

Model two is constructed analogically to model one. The time series X_t was deseasonalized in model two by subtracting the moving average of daily means. Then for $t = 1,..., T$ the 15 days two - sided moving average is calculated as

$$F_t = 1/15\sum_{i=-7}^{7}\overline{X}_{t+i} \quad (4)$$

with the series of averages calculated for each day of the year (and periodically extended accordingly)

$$\overline{X}_t = \frac{1}{n_y}\sum_{i=0}^{n_y-1} X_{(t \bmod 365)+365i} \quad (5)$$

where $n_y = \lceil T/365 \rceil$ is the number of years and leaving out the February 29th data. For F_t with $t \le 7$ and $t \ge T - 7$ appropriate adjustments were made. Optionally, the moving average smoothing can be omitted from the deseasonalization process. The deseasonalized time series X_t^d is then obtained as

$$X_t^d = X_t - F_t \quad (6)$$

The forecasts $X_{T+s+1},..., X_{T+s+h}$ are calculated as follows

- The seasonal filter is recalculated including the newly obtained observation X_{T+s}. The seasonal forecast is then $F_{((T+s+1) \bmod 365)}, ..., F_{((T+s+h) \bmod 365)}$.
- $X_1,..., X_T$ is deseasonalized using the updated seasonal filter.
- The ARFIMA forecast is calculated.
- The overall forecast is calculated by adding the ARFIMA forecast and the forecast of the seasonal component.

Model three

In the model three the non-decimated Haar à trous algorithm is used (Shensa, 1992). Applying a convolution filter $h = (0.5, 0.5)$ yields

$$s_{j+1,t} = \frac{1}{2}(s_{j,t-2^j} + s_{j,t}) \quad (7)$$

$$d_{j+1,t} = s_{j,t} - s_{j+1,t} \quad (8)$$

From Eqs. (7)–(8) can be seen that the end of the signal is not being shifted during the wavelet transform, thus the already calculated wavelet coefficients remain unchanged when new observations X_{T+1} , X_{T+2} , ... are included into the transform (Renaud et al., 2003). This makes this method especially suitable for forecasts, since the edge effects due to the usually performed circular shift of the time series applied during the wavelet transform do not occur.

In this particular case holds, $X_t = s_{J,t} + \sum_{j=1}^{J} d_{j,t}$ thus the wavelet coefficients are used directly to construct the forecasts. A linear multiscale autoregressive concept suggested in Renaud et al. (2003) is used for the forecasting (model three):

$$\hat{X}_{T+1} = \sum_{j=1}^{J}\sum_{k=1}^{A_j} a_{j,k} d_{j,T-2^j(k-1)} + \sum_{k=1}^{A_j+1} a_{J+1,k} s_{J,T-2^j(k-1)} \quad (9)$$

where A_j are the orders of the autoregressive model for each frequency interval. In this paper, $A_j = 2$ was used for all resolution levels.

Forecasts comparison

The forecasting performance is evaluated using the modified Diebold Mariano test (Diebold and Mariano, 1995; Harvey et al., 1997), the Nash-Sutcliffe coefficient (Nash and Sutcliffe, 1970) and the Theil's inequality coefficient (Theil, 1958). The model outputs are furthermore visually compared using scatter plots of measured and forecasted runoffs. For a detailed description of the tests see Appendix 2.

RESULTS

The described models are applied to a time series of mean daily runoffs of the Danube River at the gauge Kienstock near the city of Krems an der Donau in Lower Austria. The catchment area corresponding to the Kienstock gauge is 95,970km^2. The time series displays periodic behavior due to the seasonal components in the weather over the year typical of the continental climate. No trend was found in the time series. The three models were fitted for the period January 1982–December 2006 and verified for the consecutive two years.

Fig. 2 shows the series of daily mean runoffs from the Kienstock gauge used in the analyses and the periodogram of the data. The highest peak in the periodogram represents the annual periodicity in the time series.

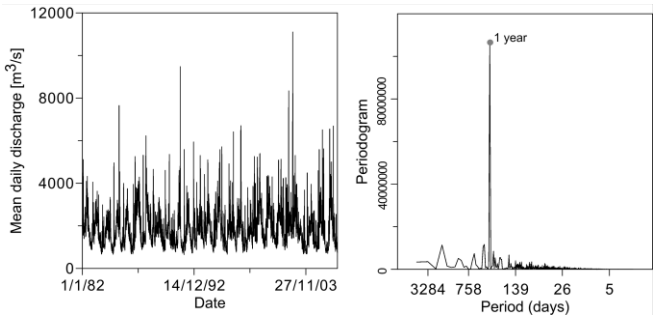

Fig. 2. Danube daily discharge at the Kienstock gauge, period 1.1.1992–31.12.2006 (left) and the periodogram of the time series (right).

Since discharge takes only positive values, the natural logarithm of the original series was used in the analysis (let us denote $X_t' = \ln X_t$) (Lohre et al., 2003) (thus the forecast was obtained as $\hat{X}_{T+s}(h) = \exp(X'_{T+s}(h))$). This transformation also brings the distribution of the data closer to the normal distribution which is assumed by the ARFIMA model.

Model fit

For the wavelet deseasonalized series (model one), the subseries $D_{8,t}$ was subtracted from the series X_t'. $D_{8,t}$ corresponds to the frequency interval $(2^{-9},2^{-8}$ which includes the annual periodicity of 365 days. A comparison of the seasonal components removed by subtracting $D_{8,t}$ (wavelet deseasonalization) and the smoothed daily averages (moving average deseasonalization) can be seen in Fig. 3. The resulting seasonal filters are rather similar for both methods. This is expected since the seasonal behavior of the discharge process is assumed to be similar every year. However, it can be seen that unlike the MA filter, the wavelet filter is changing over the years, thus reacting to changes in the driving processes in the catchment. The wavelet spectrum of the time series for the corresponding time period is depicted under the deseasonalization filters. This explains the irregularities in the wavelet deseasonalization method (for example in the year 2002) where the annual frequency is not as significant as in the rest of the time series. The wavelet spectrum and the wavelet deseasonalization, thus reflect the actual behavior of the runoff in that periods - the floods in august 2002 (counting among the most significant of 20th century (Pekárová et al., 2013) and the drought in the year 1997 (Patassiová et al., 2002). Unlike the wavelet deseasonalization, the moving average deseasonalization does not capture such irregular changes in the seasonal components which might be present in the time series.

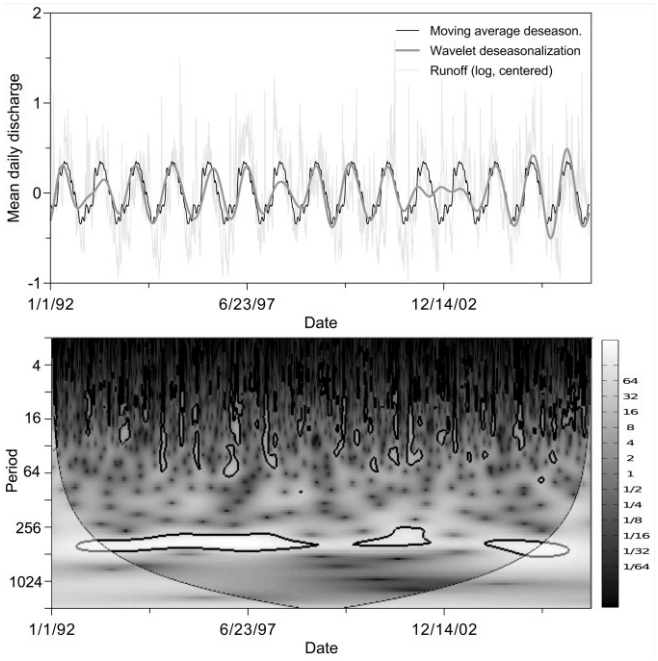

Fig. 3. The image on the top shows the series used for deseasonalization; the moving average of daily means and the wavelet filter, both for the period 1992–2006. The bottom image is the wavelet spectrum of the time series for the corresponding period. The white band in the lower part of the figure corresponds to the annual periodicity, as indicated on the vertical axis of the figure.

The change in the ACF of the time series after removing the seasonal components is shown in Fig. 4. A difference in the two deseasonalization approaches is especially visible from the periodogram figures. The wavelet deseasonalization is more ”thorough” - the frequency band around the annual periodicity of 365 days is mostly filtered out. A closer observation of the ACFs at the lags around one year shows, however, that the moving average deseasonalization was able to remove the autocorrelation better than the wavelet method for this particular area.

For the ARFIMA models various p, q combinations were fitted, based on the ACF and the partial autocorrelation function. These models were compared using the Akaike information criterion. In both cases, an ARFIMA(1,d,1) model was chosen as the most suitable one. The model parameters are shown in Table 1. The difference in the constant term c occurs since the moving average deseasonalization centers the time series, but the wavelet component has zero mean, and thus has no impact on the time series from this point of view and has to be removed later in the modelling process.

The Hurst coefficient estimates following from the model fit are derived from the respective differencing parameters of the model, obtaining $H_{model\ 1} = 0.76$ and $H_{model\ 2} = 0.83$. Since both estimates are higher than 0.5, the respective processes display long range dependence, justifying the choice of the ARFIMA model.

An inverse wavelet transform of the log daily discharges using the Haar wavelet can be seen in Fig. 5. For model 3 both J = 5 and J = 10 models were constructed, their forecasting performance was equivalent, thus the simpler model was chosen for the final comparison.

The autocorrelation functions of the residuals of all three models are in Fig. 6. In each case, the models are able to remove almost all significant autocorrelation structure.

Table 1. Parameters of the fitted ARFIMA models (see Appendix 1).

Model	d	ϕ_1	θ_1	c
1	0.26	0.73	0.28	7.44
2	0.33	0.68	0.25	0

Forecasting comparison

Based on the fitted models, one-to-ten-days ahead forecasts were constructed for the two years (730 days) following the fitting period. The comparison of the forecasting performance for all considered forecast horizons is in Table 2. In general, for a fixed horizon h the forecasts are of comparable quality when comparing the Theil’s coefficient and Nash-Sutcliffe coefficients, especially for h < 4. For 1 and 2 steps ahead forecasts all the three models deliver statistically equivalent forecasts as can be seen from the results of the modified Diebold - Mariano test. However, the forecasting performance changes with the increase of the forecasting horizon. For h = {3,... 5} the wavelet - ARFIMA (model one) outperforms the MA - ARFIMA model (model two) and for higher forecasting horizons the wavelet model (model three) as well. Furthermore for h = 10, the wavelet model performs worse than the other two considered models. As can be seen from the Nash-Sutcliffe coefficient E, with increasing forecasting horizon, the deterioration of the quality of the forecasts of the multiresolution wavelet model (model three) is faster compared to the other 2 models for h > 5. For h = 10 we have $E_{m.3} = 0.03$ which indicates forecasting with the mean of the time series is almost equivalent as the wavelet forecast. For the other two models we have $E_{m.1} = 0.12$ and $E_{m.2} = 0.07$. However, the forecasting performance is decreasing dramatically with the increase of the forecasting horizon (compare the Nash-Sutcliffe and Theil’s coefficients in Table 2). for all three models, which is not unexpected.

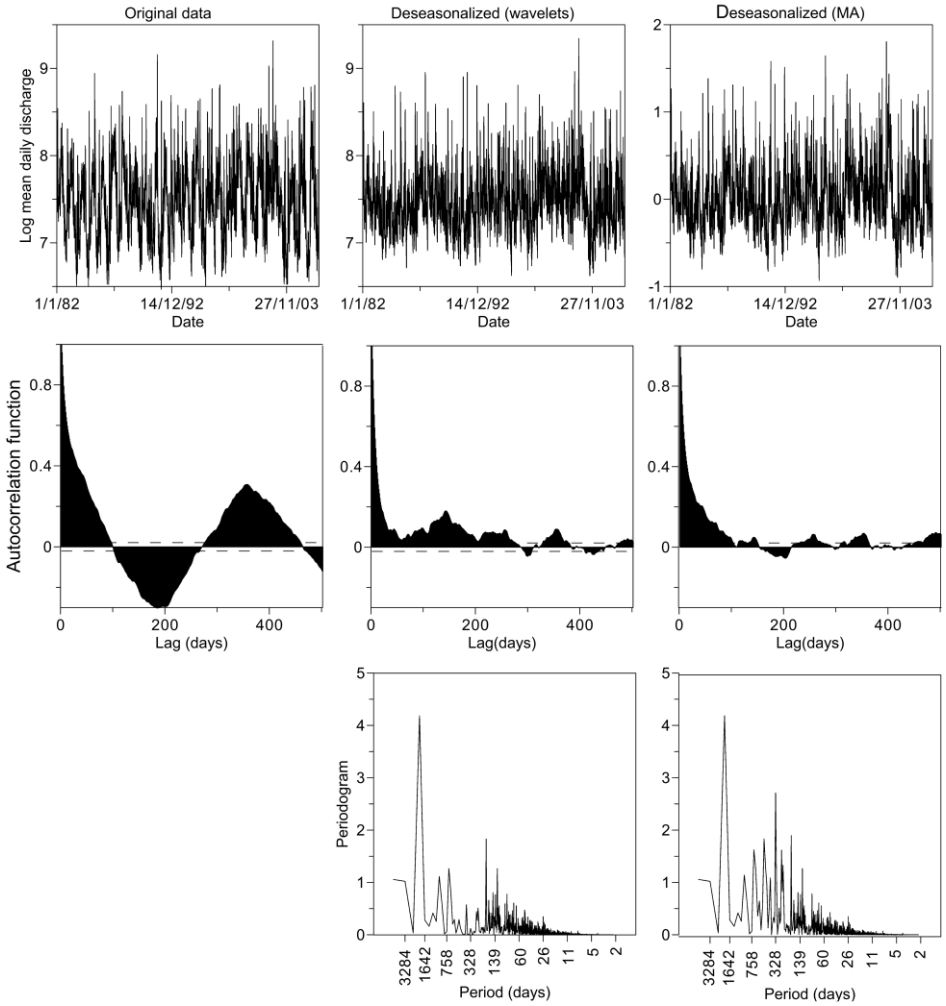

Fig. 4. Autocorrelation function of the time series. The left pictures show the (logarithm) of the original runoff time series and its autocorrelation function. The figures on the right depict the autocorrelation function after deseasonalization (using wavelets in the middle and using the moving average subtraction on the right) and the respective residual series. In the bottom of the Figure there are the periodograms calculated after the application of the respective deseasonalization method.

Both the Nash-Sutcliffe coefficient (for all models approximately 0.84) and the Theil's inequality coefficient (approximately 0.07 in all cases) indicate good forecasting performance for one-day-ahead forecasting horizon.

Scatter plots of observed versus predicted runoffs for h = {1, 3, 6, 10} can be seen in Fig. 7. These particular horizons were chosen since here the comparative forecasting performance of the respective models changes (see the MDM test in Table 2). The deterioration of the forecasting quality can be seen from the scatterplots. All scatter plots indicate a problem of the respective model when extreme runoff values (i.e. potential floods) appear in the time series.

DISCUSSION AND CONCLUSIONS

The main objective of this study was to examine, whether applying wavelets in order to model the seasonal component in a hydrological time series, is an alternative to moving average deseasonalization in combination with a long-range dependent ARFIMA model. A comparison of the forecasting performance in term of one-to-ten-steps-ahead forecasts of these two models was conducted. An additional comparison with a simple linear purely wavelet based model was provided. The models were applied to a time series of daily mean discharge of the River Danube measured at gauge Krems.

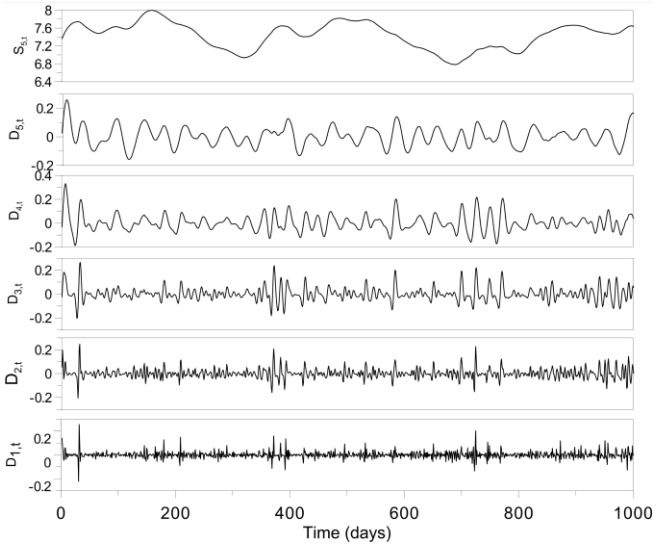

Fig. 5. The smooth and detail time series components calculated using the (inverse) Haar wavelet transform (model three).

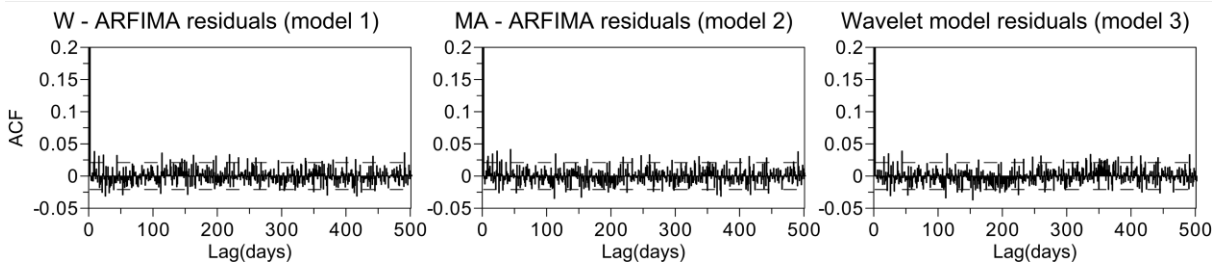

Fig. 6. Autocorrelation function of the residuals for each of the three applied models. The dashed lines depict the significance bounds.

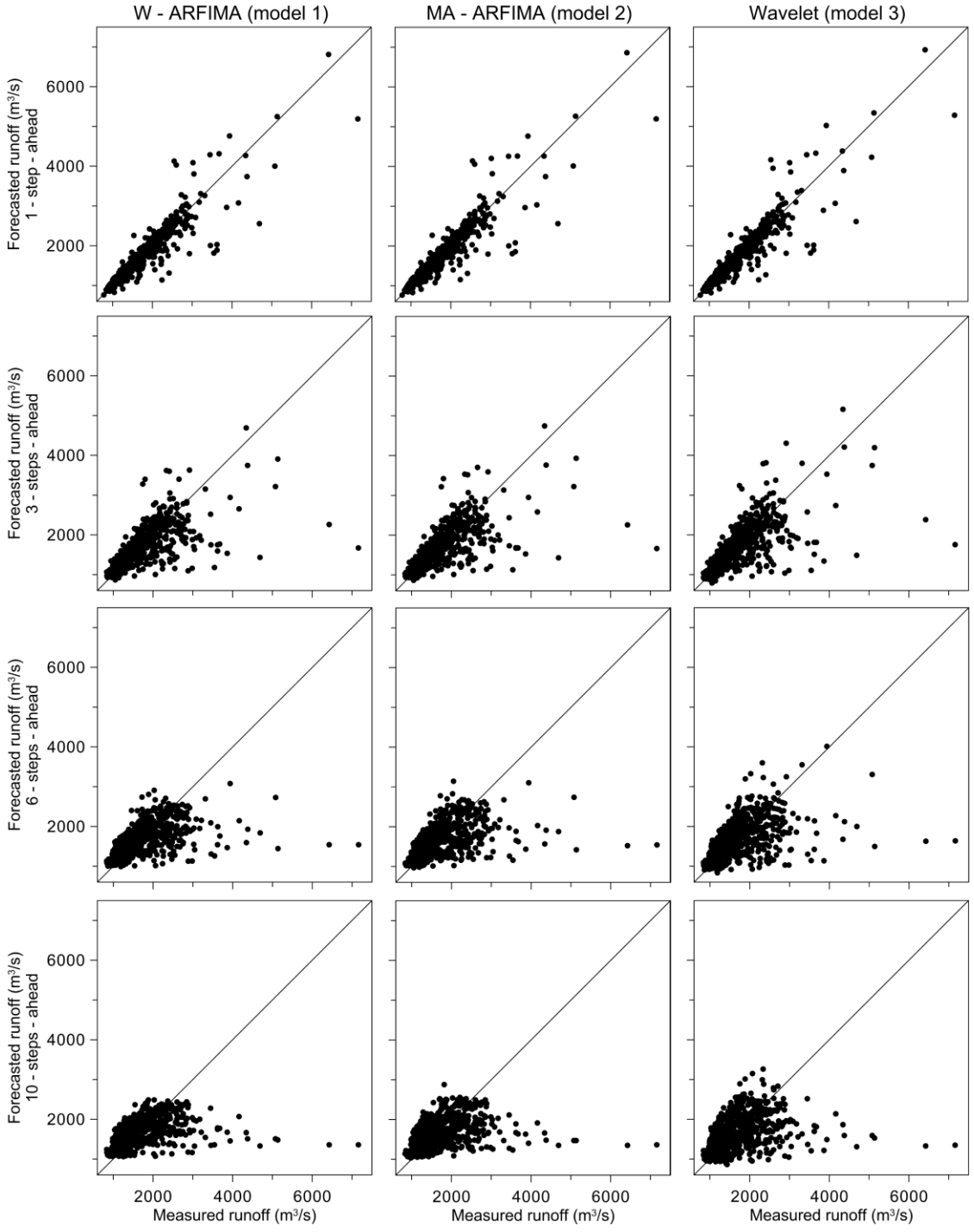

Fig. 7. Scatterplots of measured daily discharges versus the forecasted discharges using all three models. Forecasting horizons of 1, 3, 6 and 10 days are shown.

It would seem plausible that wavelets, since localized both in time and frequency thus able to capture the irregularities in the seasonal cycle better than the traditional moving average method, would provide an improvement to the traditional model. Unlike the rather generic moving average filter which reflects the average behavior of the time series on a daily basis, the wavelet deseasonalization is based on a more detailed description of the time series in the respective frequency interval, thus more reflecting on the physical behavior of the discharge. Indeed, the wavelet deseasonalization was able to capture atypical behavior, such as the floods in the year 2002.

Both of the models using the two different deseasonalization methods delivered statistically equivalent forecasts for one-and-two-days-ahead forecasts. The fact that the wavelet – an ARFIMA model did not outperform the other model for h = 1, 2 may be due to several reasons. Firstly, the wavelet transform (repeated in each day of the forecasting period) suffers from edge effects (Torrence and Compo, 1998). This has a negative impact on the forecasting performance. Secondly, a trigonometric function was fitted to the wavelet coefficients in order to model the seasonal component. The trigonometric function is periodic, thus the ability of the wavelets to capture the temporal irregularities could not be exploited in full. This effect was, however, dampened by the use of the inverse transform following the trigonometric fit. The good comparable performance of an autoregressive model compared to an ARFIMA model, even in case of long range dependence, was pointed out already by Crato and Ray (1998).

Table 2. Forecasting performance comparison - outputs from the Nash-Sutcliffe coefficient (E) and the Theil's coefficient (U) and the modified Diebold Mariano test (MDM). For the MDM test, the comparison model is given in parentheses.

	Forecasting horizon									
	1	2	3	4	5	6	7	8	9	10
W-ARFIMA										
E	0.84	0.60	0.43	0.33	0.27	0.23	0.20	0.17	0.14	0.12
U	0.07	0.12	0.14	0.15	0.16	0.16	0.17	0.17	0.17	0.18
MDM (m. 2)	0	0	1	1	1	1	1	1	1	1
MDM (m. 3)	0	0	0	0	0	1	1	1	1	1
MA-RFIMA										
E	0.84	0.60	0.42	0.31	0.24	0.20	0.17	0.13	0.10	0.07
U	0.07	0.12	0.14	0.15	0.16	0.17	0.17	0.17	0.18	0.18
MDM (m. 1)	0	0	–1	–1	–1	–1	–1	–1	–1	–1
MDM (m. 3)	0	0	0	0	0	0	0	0	0	1
Wavelets										
E	0.84	0.60	0.42	0.31	0.24	0.19	0.15	0.11	0.06	0.03
U	0.07	0.12	0.14	0.15	0.16	0.17	0.17	0.18	0.18	0.18
MDM (m. 1)	0	0	0	0	0	–1	–1	–1	–1	–1
MDM (m. 2)	0	0	0	0	0	0	0	0	0	–1

The linear wavelet based model performed well (as indicated by both Nash-Sutcliffe coefficient and Theil's one) for short forecasting horizon which is in general accordance with the literature (Renaud et al., 2003). The quicker deterioration of the wavelet based model compared with the other two ARFIMA models might indicate that incorporating long range dependence even if considering daily time steps could be profitable. Similarly, Prass et al. (2012) showed improvement in short term forecasting when incorporating long range dependence into a model on data with monthly time step.

For longer forecasting horizons (h > 2) the combined wavelet – an ARFIMA model outperformed the other two models. The quality of the forecasts decreased significantly with the increase of the forecasting horizons for all three models, however, this was especially pronounced in the case of the linear wavelet model for h > 5. This is in accordance with general properties of time series forecasting (Brockwell and Davis, 2002). It can be concluded that for longer forecasting horizons, the quality of the forecasts of the new wavelet, an ARFIMA model is statistically better than the traditional combination of moving average deseasonalization with ARFIMA. For higher forecasting horizons the wavelet, an ARFIMA model outperforms the multiresolution wavelet model as well (according to the Diebold Mariano test). Thus the wavelet deseasonalization offers improvement in time series forecasting for time series with long range dependence for higher forecasting horizons.

Finally, it should be noted than none of the three models was able to fully remove autocorrelation from the squared residuals after the model fit. This autocorrelation usually indicates heteroscedasticity in the time series, thus the concept of the wavelet deseasonalization may be explored further in combination of other possibly suitable model, such as a fractionally integrated generalized autoregressive conditional heteroscedasticity (Engle, 1982; Modarres and Ouarda, 2012) model type.

Acknowledgement. We would like to acknowledge financial support from the Austrian Science Funds (FWF) as part of the Vienna Doctoral Programme on Water Resource Systems (DK-plus W1219-N22). Furthermore the research summarized in this paper was supported by the grants APVV 0303-11 and Czech Science Foundation P402/12/G097.

REFERENCES

Adamowski, J.F., 2008. Development of a short-term river flood forecasting method for snowmelt driven floods based on wavelet and cross-wavelet analysis. J. Hydrol., 353, 247–266.

Andreo, B., 2006. Climatic and hydrological variations during the last 117-166 years in the south of the Iberian Peninsula, from spectral and correlation analyses and continuous wavelet analyses. J. Hydrol., 324, 24–39.

Beran, J., 1994. Statistics for long - memory processes. Chapman and Hall, New York.

Blöschl, G., Reszler, C., Komma, J., 2007. A spatially distributed flash flood forecasting model. Environ. Modell. Softw., 23, 464–478.

Box, G.E.P., Jenkins, G.M., 1976. Time series analysis forecasting and control. Holden-Day, San Francisco, USA.

Brockwell, P., Davis, R.A., 2002. Introduction to time Series and forecasting. Springer Verlag, New York, USA.

Burlando, P., Rosso, R., Cadavid, L.G., Salas, J.D., 1993. Forecasting of short-term rainfall using ARMA models. J. Hydrol., 144, 193–211.

Daubechies, I., 1992. Ten Lectures on Wavelets. Society for Industrial and Applied Mathematics, Philadephia, USA.

Crato, N., Ray, B.K., 1998. Model selection and forecasting for long-range dependent processes. Journal of Forecasting, 15, 107–125.

Diebold, F.X., Mariano, R.S., 1995. Comparing predictive accuracy. Journal of Business and Economic Statistics, 13, 253–263.

Harvey, D.I., Leybourne, S.J., Newbold, P., 1997. Testing the equality of prediction mean squared errors. International Journal of Forecasting, 13, 281–291.

Dou, H., Chan, Y.Q., 1998. Optimal Features Extraction of Noisy Sinusoidal Signals Using Two-Stage Linear Least Squares Fitting. Technical report, Mechatronics and Automation Laboratory, National University of Singapore.

Ehsanzadeh, E., Adamowski, K., 2010. Trends in timing of low stream flows in Canada: impact of autocorrelation and long - term persistence. Hydrol. Process., 24, 970–980.

Doukhan, P., Oppenheim, G., Taqqu, M. S., 2003. Long-range dependence. Birkhäuser, Boston, USA.

Engle, R.F., 1982. Autoregressive Conditional Heteroscedasticity with Estimates of the Variance of United Kingdom Inflation. Econometrica, 50, 987–1008.

Gencay, R., Selcuk, F., Whitcher, B., 2001. Differentiating intraday seasonalities through wavelet multi - scaling. Physica A, 289, 543 – 556.

Grinsted, A., Moore, J.C., Jevrejeva, S., 2004. Application of the cross wavelet transform and wavelet coherence to geophysical time series. Nonlinear Proc. Geoph., 11, 561–566.

Hipel, K.W., McLeod, A.I., 1994. Time Series Modelling of Water Resources and Environmental Systems. Elsevier, Amsterdam.

Jain, S.K., Sudheer, K.P., 2012. Fitting of hydrologic models: a close look at the nash–sutcliffe index. J. Hydrol. Eng., 13, 981–986.

Komorník, J., Komorníková, M., Mesiar, R., Szökeová, D., Szolgay, J., 2006. Comparison of forecasting performance of nonlinear models of hydrological time series. Phys. Chem. Earth, 18, 1127–1145.

Komorníková, M., Szolgay, J., Svetlíková, D., Szökeová, D., Jurčák, S., 2008. A hybrid modelling framework for forecasting monthly reservior inflows. J. Hydrol. Hydromech., 56, 145–162.

Koop, G., Ley, E., Osiewalski, J., Steel, M.F.J., 1997. Bayesian analysis of long memory and persistence using ARFIMA models. J. Econometrics, 76, 149–169.

Koscielny-Bunde, E., Kantelhardt, J.W., Braun, P., Bunde, A., Havlin, S., 2006. Long - term persistence and multifractality of river runoff records: Detrended fluctuation studies. J. Hydrol., 322, 120–137.

Lohre, M., Sibbertsen, P., Könning, T., 2003. Modeling water flow of the Rhine River using seasonal long memory. Water Resour. Res., 39, 1132.

Lye, L.M., Lin, Y., 1994. Long - term dependence in annual peak flows of Canadian rivers. J. Hydrol., 160, 89–103.

Maier, H.R., Dandy, G.C., 2000. Neural networks for the prediction and forecasting of water resources variables: a review of modelling issues and applications. Environ. Modell. Softw., 15, 101–124 .

Mallat, S., 1998. A Wavelet Tour of Signal Processing Academic Press, New York.

Nelson, M., Hill, T., Remus, W., O'Connor, M., 1999. Time series forecasting using neural networks: Should the data be deseasonalized first? Journal of Forecasting, 18, 359–367.

Modarres, R., Ouarda, T.B.M.J., 2012. Generalized autoregressive conditional heteroscedasticity modelling of hydrologic time series. Hydrol. Process., 27, 22, 3174–3191.

Montanari, A., Rosso, R., Taqqu, M. S., 1997. Fractionally differenced ARIMA models applied to hydrologic time series: Identification, estimation, and simulation. Water Resour. Res., 33, 1035–1044.

Montanari, A., Taqqu, M., Teverovski, V., 1999. Estimating long-range dependence in the presence of periodicity: an empirical study. Math. Comput. Model., 29, 217–228.

Nash, J.E., Sutcliffe, J.V., 1970. River flow forecasting through conceptual models part I - A discussion of principles. J. Hydrol., 10, 282–290.

Ooms, M., Franses, P.H., 2001. A seasonal periodic long memory model for monthly river flows. Environ. Modell. Softw., 16, 559–569.

Pasquini, A.I., Depetris, P.J., 2010. ENSO - triggered exceptional flooding in the Parana River: Where is the excess water coming from? J. Hydrol., 383, 186–193.

Patassiová, M., Klementová, E., Litschmann, T., Čistý, M., 2002. Analysis of the drought and influence of the precipitation on its occurrence during spring months. Acta Hydrologica Slovaca, 3, 94–101. (In Slovak.)

Pelletier, J.D., Turcotte, D.L., 1997. Long-range persistance in climatological and hydro- logical time series: analysis, modeling and application to drought hazard assessment. J. Hydrol., 203, 198–208.

Pekárová, P., Halmová, D., Bačová Mitková, V., Miklánek, P., Pekár, J., Škoda, P., 2013. Historic flood marks and flood frequency analysis of the Danube River at Bratislava, Slovakia. J. Hydrol. Hydromech., 61, 326–333.

Prass, T.S., Bravo, J.M., Clarke, R.T., Collischonn, W., Lopes, S.R.C., 2012. Comparison of forecasts of mean monthly water level in the Paraguay River, Brazil, from two fractionally differenced models. Water Resour. Res., 48, W05502.

Quimpo, R.G., 1969. Reduction of serially correlated hydrologic data. Bulletin of the International Association of Scientific Hydrology, 4, 111–118.

Renaud, O., Starck, J., Murtagh, F., 2003. Prediction based on multiscale decomposition. Int. J. Wavelets Multi., 1, 217–232.

Reszler, C., Blöschl, G., Komma, J., 2008. Identifying runoff routing parameters for operational flood forecasting in small to medium sized catchments. Hydrological Sciences Journal, 53, 112–129.

Shensa, M.J., 1992. Discrete wavelet transforms: Wedding the à trous and Mallat algorithms. In: IEEE Transactions on Signal Processing, 40, 2464–2482.

Starck, J.L., Murtagh, F., Bijaoui, A., 1998. Image processing and data analysis: The multiscale approach. Cambridge University Press, Cambridge, United Kingdom.

Teverovsky, V., Taqqu, M. S., Willinger, W., 1995. Estimator for long-range dependence: an empirical study. Fractals, 3, 785–798.

Theil, H., 1958. Economic Forecasting and Policy. North Holland, Amsterdam.

Thuillard, M., 2002. A review of wavelet networks, wavenets, fuzzy wavenets and their applications. Advances in computational intelligence and learning, 18, 43–60.

Torrence, C., Compo, G.P., 1998. A practical guide to wavelet analysis. B. Am. Meteorol. Soc., 78, 61–78.

Torrence, C., Webster, P.J., 1999. Interdecadal Changes in the ENSO–Monsoon System. J. Climate, 12, 2679–2690.

Yousefi, S., Weinreich, I., Reinarz, D., 2005. Wavelet-based prediction of oil prices. Chaos Soliton. Fract., 25, 265–275.

Wei, S., Song, J., Khan, N.I., 2012. Simulating and predicting river discharge time series using a wavelet-neural network hybrid modelling approach. Hydrol. Process., 26, 28–296.

Zealand, C.M., Burn, D.H., Simonovic, S.P., 1999. Short term streamflow forecasting using artificial neural networks. J. Hydrol., 214, 32–48.

APPENDIX 1

Long range dependence and ARFIMA(p,d,q) model

A time series X_t, $t = 1,...T$ with long range dependence can be characterized by a hyperbolic decrease with the time lag τ of the autocorrelation function $\rho_\tau = Corr[X_t, X_{t+\tau}]$

$$\rho_\tau \approx C\tau^{2H-2} \qquad \tau \to \infty \tag{10}$$

where C is a constant and H is the Hurst coefficient. In case of long range dependence (or long term persistence, long memory) $H > 0.5$ (in general $H \in [0,1]$). There are numerous methods for estimating the Hurst coefficient (Teverovsky et al., 1995). In this paper we will estimate the Hurst coefficient as a part of the later described ARFIMA model (Beran, 1994).

In order to capture long range dependence in the modelling process, an autoregressive fractionally integrated moving average model ARFIMA(p,d,q) may be used:

$$(1-\sum_{i=1}^{p}\phi_i B^i)(1-B)^d X_t = (1+\sum_{j=1}^{q}\theta_j B^j)\varepsilon_t + c \tag{11}$$

where B is the backshift operator, ϕ_i and ϕ_j are the parameters of the autoregressive and moving average components of the model, c is a constant and d is the rational fractional parameter and $H = d + 0.5$. Thus in case of long term persistent processes holds $d \in (0,0.5)$.

APPENDIX 2

The modified Diebold Mariano Test

Consider two competing models A and B. The modified Diebold Mariano test tests the null hypothesis H_0: A, B produce equally accurate h-steps-ahead forecasts. The test statistics is given by

$$MDM = \left(\frac{m+1-2h+h(h+1)/m}{m}\right)^{1/2} \frac{\bar{d}}{(mV(\bar{d}))^{1/2}} \tag{12}$$

where m is the length of the interval, on which the (out-of sample) h-steps-ahead forecasts are made (h is the forecasting horizon) and $\bar{d} = 1/m\sum_{s=0}^{m} d_s = 1/m\sum_{s=0}^{m}(\hat{e}^A_{T+s}(h) - \hat{e}^B_{T+s}(h))^2$ are the model errors, forecasts being denoted as $\hat{X}^A_{T+s}(h)$ for $s = 0, ..., m$ (i.e. $\hat{X}_{T+s}(h)$ is the forecasted runoff for the day $T + s + h$ with h days forecasting horizon and the forecasting threshold $T + s$). $V(\bar{d})$ is the estimate of the variance of d_s. The test output has three possible entry values: 0 (statistically equivalent performance), –1 or 1 representing significantly worse or better performance of model A compared to B respectively.

The Nash-Sutcliffe coefficient

The Nash-Sutcliffe coefficient E is widely used in hydrology to assess the forecasting performance (Jain and Sudheer, 2012; Nash and Sutcliffe, 1970) and it is defined as

$$E = 1 - \frac{\sum_{s=0}^{m}\hat{e}^2_{T+s}(h)}{\sum_{s=0}^{m}(X_{T+s+h} - \bar{X})^2} \tag{13}$$

where $\bar{X} = 1/T\sum_{t=1}^{T} X_t$. In general $E \in (-\infty, 1]$, higher values indicating better performance, $E = 1$ meaning a perfect forecast.

The Theil coefficient

The Theil inequality coefficient U is defined as

$$U = \frac{\sqrt{\frac{1}{m+1}\sum_{s=0}^{m}\hat{e}^2_{T+s}(h)}}{\sqrt{\frac{1}{m+1}\sum_{s=0}^{m}\hat{X}^2_{T+s}(h)} + \sqrt{\frac{1}{m+1}\sum_{s=0}^{m}X^2_{T+s+h}}} \tag{14}$$

for the Theil coefficient holds $U \in [0,1]$, the quality of the forecast increasing with the decreasing U.

Received 11 October 2013
Accepted 19 December 2013